Design, Synthesis, and Evaluation of a Novel 4-Aminomethyl-4-fluoropiperidine as a T-Type Ca^{2+} Channel Antagonist

William D. Shipe,*[,†] James C. Barrow,[†] Zhi-Qiang Yang,[†] Craig W. Lindsley,[†,●] F. Vivien Yang,[†] Kelly-Ann S. Schlegel,[†] Youheng Shu,[†] Kenneth E. Rittle,[†] Mark G. Bock,[†,∞] George D. Hartman,[†] Cuyue Tang,[‡] Jeanine E. Ballard,[‡] Yuhsin Kuo,[‡] Emily D. Adarayan,[‡] Thomayant Prueksaritanont,[‡] Matthew M. Zrada,[‡] Victor N. Uebele,[§] Cindy E. Nuss,[§] Thomas M. Connolly,[§,⊥] Scott M. Doran,[§] Steven V. Fox,[§] Richard L. Kraus,[§] Michael J. Marino,[||,×] Valerie Kuzmick Graufelds,[||] Hugo M. Vargas,[#,◆] Patricia B. Bunting,[#] Martha Hasbun-Manning,[#] Rose M. Evans,[#] Kenneth S. Koblan,[◇] and John J. Renger[§]

Departments of Medicinal Chemistry, Depression and Circadian Disorders, Parkinson's Disease, Drug Metabolism, and Safety and Exploratory Pharmacology, Merck Research Laboratories, WP14-1, P.O. Box 4, Sumneytown Pike, West Point, Pennsylvania 19486

Received April 11, 2008

Abstract: The novel T-type antagonist (*S*)-**5** has been prepared and evaluated in in vitro and in vivo assays for T-type calcium ion channel activity. Structural modification of the piperidine leads **1** and **2** afforded the fluorinated piperidine (*S*)-**5**, a potent and selective antagonist that displayed in vivo CNS efficacy without adverse cardiovascular effects.

Calcium is an important physiological signaling molecule, and control of intracellular calcium concentration is a tightly regulated process. Calcium ions (Ca^{2+}) can be released from intracellular stores or enter the cell via ligand-gated or voltage-gated calcium channels, initiating a wide range of physiological responses.[1] Historically, voltage-gated calcium channels have been divided by functional descriptors of the Ca^{2+} currents (L-type, N-type, T-type, etc.), but more recently molecular cloning of the critical pore forming α subunit has resulted in three main classes denoted $Ca_v1.x$ (L-type), $Ca_v2.x$ (N, P/Q, R-type), and $Ca_v3.x$ (T-type).[2] The $Ca_v3.x$ family has three members ($Ca_v3.1$, $Ca_v3.2$, and $Ca_v3.3$), and these channels activate at more negative membrane potential than members of the $Ca_v1.x$ and $Ca_v2.x$ families and produce smaller and more transient currents. They are widely expressed in CNS and peripheral tissues and may have potential for the treatment of various indications such as hypertension, epilepsy, pain, regulation of arousal states, tinnitus, and cancer.[3] In the brain, T-type channels are found in the thalamic and cortical regions where they have an important role in the function of the thalamocortical loop, a neural network structure implicated in absence epilepsy, arousal state, and movement disorders such as essential tremor.[4]

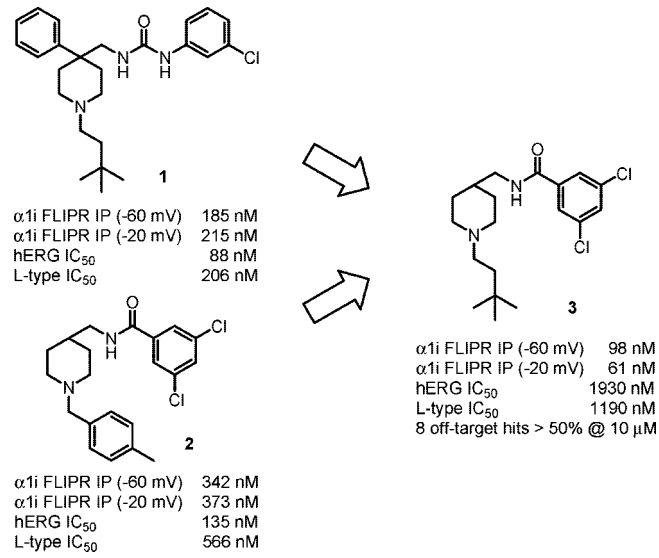

Figure 1. Profiles of 4-aminomethyl piperidine leads **1**−**3**.

Mibefradil, often described as the first selective T-type antagonist, demonstrated efficacy as an antihypertensive.[5] Shortly after its introduction, mibefradil was withdrawn from the U.S. market in 1998 because of drug−drug interactions,[6] but in lieu of other compounds, it remains the prototype T-type calcium channel blocker. Additionally, ethosuximide has T-type antagonist properties (among others) and is used to suppress absence seizures.[7] Potent and selective agents are needed to better elucidate the true functional role of T-type calcium channels in these and other disease states. With increasing knowledge of the localization, function, and properties of T-type calcium channels, there has been heightened activity for the discovery of novel inhibitors in recent years.[8] Here, we detail the discovery of a novel, orally bioavailable piperidine T-type calcium channel antagonist that evolved via optimization of piperidines **1** and **2** and its in vivo evaluation in cardiovascular and CNS models.

Screening efforts identified piperidines **1** and **2** as T-type Ca^{2+} channel antagonists (Figure 1). Their ability to block the $Ca_v3.3$ (α1I) channel was assessed using a high-throughput cell-based calcium flux assay (FLIPR[a]) at a membrane potential of −20 mV (depolarized) or −60 mV (hyperpolarized).[9] High-voltage activated Ca^{2+} channel antagonists can have preferential affinity for one state over another, and these properties can profoundly affect the efficacy and safety profiles of the compounds.[10] Although it is unknown whether these properties would impact the physiological effect of T-type antagonists, the state-dependent properties of all described compounds were also characterized by standard voltage-clamp electrophysiological assays. The compounds were counterscreened for activity on

* To whom correspondence should be addressed. Telephone: 215-652-6527. Fax: 215-652-6345. E-mail: william_shipe@merck.com.
† Department of Medicinal Chemistry.
● Current address: Vanderbilt University.
∞ Current address: Novartis Institutes for BioMedical Research, Inc.
‡ Department of Drug Metabolism.
§ Department of Depression and Circadian Disorders.
⊥ Current address: Wyeth Pharmaceuticals.
|| Department of Parkinson's Disease.
× Current address: Cephalon, Inc.
Department of Safety and Exploratory Pharmacology.
◆ Current address: Amgen, Inc.
◇ Basic Research Administration, Merck Research Laboratories, Rahway, NJ.

[a] Abbreviations: CSF, cerebrospinal fluid; DMF, dimethylformamide; ECG, electrocardiography; EEG, electroencephalography; FLIPR, fluorometric imaging plate reader; hERG, human ether-a-go-go-related gene; HOBt, *N*-hydroxybenzotriazole; HR, heart rate; MAP, mean arterial blood pressure; MP-$BH(OAc)_3$, macroporous polystyrene-bound triacetoxyborohydride; MP-carbonate, macroporous polystyrene-bound carbonate; PS-carbodiimide, polystyrene-bound carbodiimide; WAG/Rij, Wistar albino Glaxo/Rijswijk.

10.1021/jm800419w CCC: $40.75
Published on Web 06/10/2008

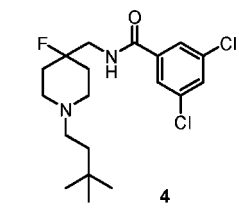

4

α1i FLIPR IP (-60 mV) 64 nM
α1i FLIPR IP (-20 mV) 66 nM
hERG IC_{50} 2220 nM
L-type IC_{50} 940 nM

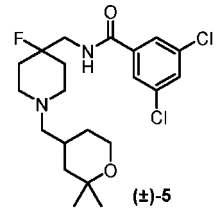

(±)-5

α1i FLIPR IP (-60 mV) 333 nM
α1i FLIPR IP (-20 mV) 145 nM
hERG IC_{50} 8410 nM
L-type IC_{50} 5810 nM

Figure 2. Profiles of piperidines **4** and **5**.

Scheme 1[a]

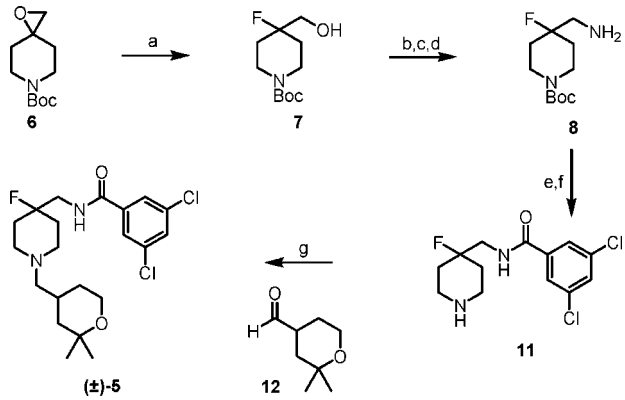

[a] Conditions: (a) 70% HF·pyridine, −10 °C → room temp; (b) *p*-TsCl, pyridine, 0 °C → room temp; (c) potassium phthalimide, DMF, 150 °C; (d) ethanolamine, 60 °C; (e) HOBt, 3,5-dichlorobenzoic acid, *i*-Pr_2EtN, PS-carbodiimide, then MP-carbonate; (f) 4 N HCl/dioxane, CH_2Cl_2; (g) **12**, MP-$BH(OAc)_3$, CH_2Cl_2.

the hERG K^+ and L-type Ca^{2+} channels using binding assays.[11,12] While **1** and **2** showed good T-type potency, a concern was the lack of selectivity observed with respect to the hERG and L-type ion channels. Blocking hERG or L-type ion channels could have unwanted cardiac effects for a CNS therapeutic agent; therefore, an early goal of the program was to improve this selectivity margin.

Initial SAR showed the neohexyl group of **1** and the 3,5-dichlorobenzoyl group of **2** to be preferred structural features from a potency viewpoint. Combining those structural elements of these leads about a 4-aminomethylpiperidine scaffold produced **3**, which showed improved T-type potency and selectivity with respect to the hERG and L-type ion channels. However, submission of the compound to a broad external screen revealed eight off-target activities with greater than 50% activity at 10 μM, reflecting its moderate selectivity versus other ion channels and GPCRs.

Fluorinated piperidine analogues were then prepared. The potential benefit of this strategy was 2-fold: (1) by reduction of the basicity of the ring nitrogen atom, the ancillary pharmacological profile might be improved; (2) the fluorinated piperidine ring might exhibit enhanced metabolic stability.[13] Compound **4**, bearing a fluorine atom at the 4-position, possessed a potency and selectivity profile similar to those of **3** (Figure 2), but improved selectivity was observed by maintaining this fluorine and varying the N-substituent. After extensive investigation, the tetrahydropyran (±)-**5** displayed the best improvement on the ion channel selectivity over analogues **3** and **4**.

The synthesis of (±)-**5** proceeded as outlined in Scheme 1. Regioselective epoxide opening of **6**[14] with HF·pyridine yielded the fluorinated alcohol **7**.[15] A straightforward three-step sequence was employed to convert **7** to primary amine **8**.[16] Amide **11** was obtained by carbodiimide-mediated coupling of **8** to 3,5-dichlorobenzoic acid and subsequent removal of the *tert*-butyloxycarbonyl protective group. Reductive amination with tetrahydropyranyl aldehyde **12**[17] provided the racemic tertiary amine **5**.

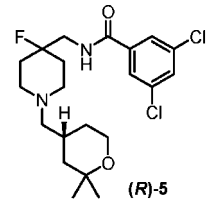

(*R*)-5

α1i FLIPR IP (-60 mV) 297 nM
α1i FLIPR IP (-20 mV) 94 nM
hERG IC_{50} 5010 nM
L-type IC_{50} 5490 nM
WAG/Rij % inhibition 63%

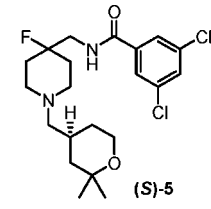

(*S*)-5

α1i FLIPR IP (-60 mV) 181 nM
α1i FLIPR IP (-20 mV) 84 nM
hERG IC_{50} 3790 nM
L-type IC_{50} 6330 nM
WAG/Rij % inhibition 81%
4 off-target hits > 50% @ 10 μM

Figure 3. Profiles of piperidines (*R*)-**5** and (*S*)-**5**.

Racemic (±)-**5** was resolved by HPLC with a ChiralPak AD column so that the biological activities of the enantiomers could be individually evaluated. Little distinction could be made between (*R*)-**5** and (*S*)-**5**[18] on the basis of ion channel data (Figure 3), but (*S*)-**5** was consistently superior in a WAG/Rij rat model of absence epilepsy (vide infra) and was selected for full characterization.

In agreement with the profile observed in the calcium flux assays, the in vitro potencies of (*S*)-**5** determined in a standard voltage-clamp electrophysiological assay at membrane holding potentials of −80 and −100 mV (115 and 84 nM, respectively) confirmed that compounds in this piperidine series are state-independent antagonists. Similar electrophysiology experiments with $Ca_v3.1$ (α1G, 93 nM at −100 mV) and $Ca_v3.2$ (α1H, 196 nM at −100 mV) indicated that the compound potently inhibits all T-type family members.

The pharmacokinetic parameters for (*S*)-**5** following intravenous and oral doses in preclinical species are shown in Table 1. The compound exhibited significant species differences in clearance and volume of distribution but relatively short half-life (∼2−5 h) across species. The oral bioavailability of (*S*)-**5** was reasonably good (>35%) in all species.

P-Glycoprotein (P-gp) mediated transport of (*S*)-**5** was found to be minimal (B-A/A-B ≤ 2), and the compound showed good passive cellular permeability ($P_{app} = 34 \times 10^{-6}$ cm/s). Consistent with the in vitro data, (*S*)-**5** showed good brain penetration in rats (brain/plasma concentration ratio of 6.0 and CSF/unbound plasma ratio of 2.8 at 9 h after dosing), supporting its potential therapeutic use as a CNS agent.

To investigate the in vivo CNS activity of these compounds, we employed a genetic model of absence epilepsy using Wistar albino Glaxo rats bred in Rijswijk, The Netherlands (WAG/Rij). The WAG/Rij rats display cortical EEG patterns and physical behaviors characteristic of an epileptic condition, including frequent seizures.[19] Since T-type calcium channels are involved in the regulation of thalamocortical rhythms, measurement of EEG in these animals serves as a relevant pharmacodynamic readout of brain penetration and T-type channel activity. (*S*)-**5** exhibited a dose- and exposure-dependent decrease in the total seizure time during the 4 h period following oral dosing (Figure 4). Notably, (*S*)-**5** demonstrated robust CNS efficacy in this model at a dose of 10 mg/kg with a plasma level of 1 μM.

Another pathophysiological condition that may result from thalamocortical dysfunction is essential tremor;[20] therefore, (*S*)-**5**

Table 1. Pharmacokinetic Profile of (*S*)-**5**

			iv (in DMSO)			po (in 1% methylcellulose)			
species	plasma protein binding (% bound)	dose (mg/kg)	CL (mL/min/kg)	$t_{1/2}$ (h)	V_{dss} (L/kg)	C_{max} (μM)	T_{max} (h)	AUC_{0-24h} (μM·h)	F (%)
rat	94.3	1	75 ± 21	1.8 ± 0.1	10 ± 2				
		10				0.48 ± 0.12	0.7 ± 0.3	1.94 ± 0.43	36 ± 8
dog	99.0	0.5	2.3	4.7	1.0				
		1				2.18 ± 1.97	3.1 ± 4.3	15.8 ± 10.9	87 ± 64
monkey	97.5	0.5	13.6	3.3	3.8				
		2				0.58	1.5	3.2	44

was also evaluated in the rat harmaline model[21] of essential tremor. Harmaline-induced tremor activity in the 6−12 Hz range was monitored and quantified to assess tremor suppression. (*S*)-**5** was found to significantly reduce tremor activity in a dose-dependent manner (Figure 5), suggesting a possible role for T-type antagonists in the treatment of movement disorders such as essential tremor.

To gain further insight into potential ancillary pharmacology, (*S*)-**5** was submitted to a large external screen, which revealed only four off-target activities with greater than 50% activity at 10 μM. Most prominent was σ receptor binding (<100 nM), but follow-up in a vas deferens functional assay[22] revealed only weak antagonist activity (30% at 30 μM). Also noted was sodium channel site 2 binding (IC_{50} = 1.9 μM), but voltage clamp studies with the $Na_v1.5$ sodium channel showed an IC_{50} of 84 μM.[23] (*S*)-**5** also showed little inhibition of $Ca_v2.2$ in a counterscreen (18% inhibition at 10 μM).[24] hERG potassium channel binding was also evident in the external screen (IC_{50} = 2.9 μM), so we examined the effect of compound on cardiovascular function in a conscious dog model.[25] Three dogs were infused intravenously with (*S*)-**5** first at a rate of 1.29 (mg/kg)/60 min and then 4.30 (mg/kg)/60 min, resulting in mean plasma levels of 1.5 ± 0.3 μM at the end of the first infusion and 4.6 ± 1.7 μM at the end of the second. No behavioral effects were noted during the study, and there were no significant changes in mean arterial blood pressure (Figure 6), heart rate (Figure 7), or ECG intervals (PR, QRS, QT, and QTc).

Since T-type calcium channels are present in renal vascular and tubular tissues,[26] (*S*)-**5** was evaluated for side effects on renal function. Four dogs were administered a single oral dose (20 mg/kg) of (*S*)-**5** and observed for 3 h after treatment.[27] No effects were observed on glomerular filtration rate, effective

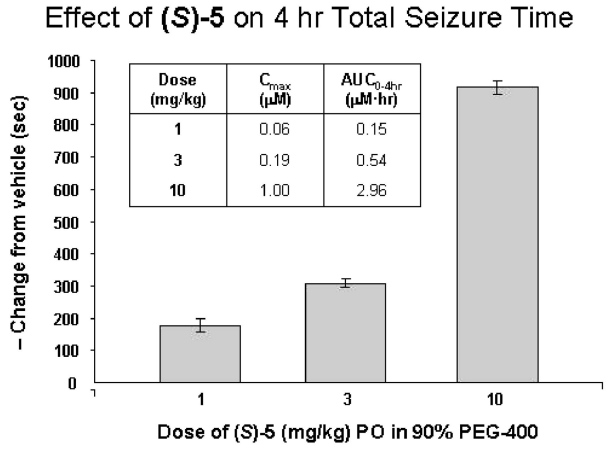

Figure 4. Dose−response of (*S*)-**5** in WAG/Rij rat model of absence epilepsy, $n \geq 6$ rats per dose with PK taken from satellite animals, $n = 3$ per group except 3 mg/kg group where $n = 1$.

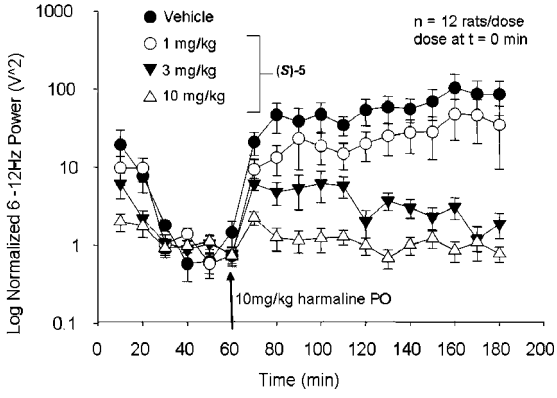

Figure 5. Dose−response of (*S*)-**5** in harmaline-induced rat model of essential tremor.

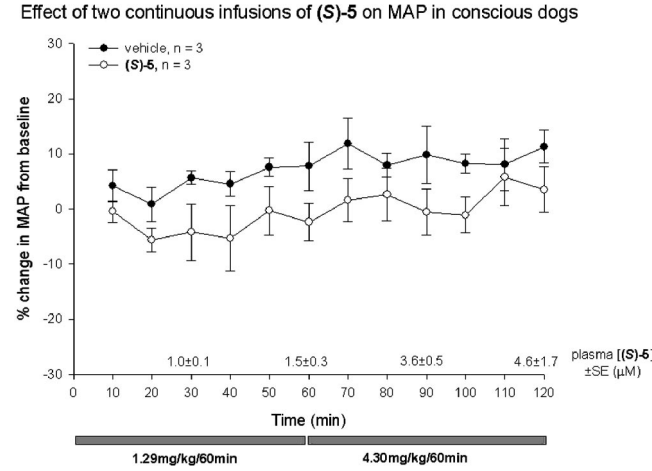

Figure 6. Effect of (*S*)-**5** on mean arterial blood pressure (MAP) in conscious dogs.

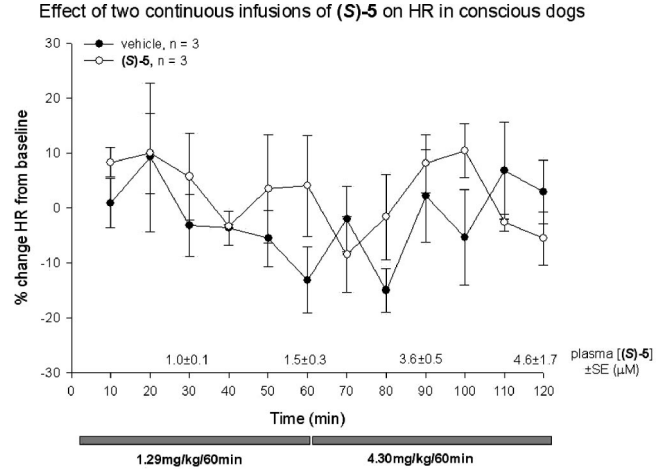

Figure 7. Effect of (*S*)-**5** on heart rate (HR) in conscious dogs.

renal plasma flow, urine flow, urinary excretion of sodium and potassium, or plasma electrolytes. While blood pressure and ECG intervals were unaffected in this assay, increased heart rate and minor behavioral changes (panting) were observed. Peak plasma concentrations of (*S*)-**5** were 34.5 ± 11.0 μM during the experiment.

In conclusion, we identified (*S*)-**5**, a potent and selective T-type calcium channel antagonist, starting from 1,4-disubstituted piperidine HTS leads. The introduction of a fluorine atom at the 4-position served to improve the ancillary pharmacological profile and to enhance metabolic stability. Robust efficacy was seen in WAG/Rij epilepsy and harmaline-induced tremor models at plasma levels well below the no effect level seen in cardiovascular dog experiments. This suggests a good margin between CNS and peripheral effects of selective T-type calcium channel antagonists. Compounds such as (*S*)-**5** hold promise for the treatment of a diverse set of neurological indications without adversely affecting cardiovascular function.

Acknowledgment. We thank Carl F. Homnick, David D. Wisnoski, Wei Lemaire, Scott D. Mosser, Rodney A. Bednar, Charles W. Ross, III, Joan S. Murphy, Kevin B. Albertson, William H. Leister, Ray T. McClain, Anna Dudkina, Emily Wang, Debra McLoughlin, and Susan Garson for technical support of this work.

Supporting Information Available: Spectral and analytical data for new compounds, a scheme detailing the preparation of **5**, FLIPR assay protocol, $Na_v1.5$ electrophysiology measurements, dog renal function assay protocol, and expanded references. This material is available free of charge via the Internet at http://pubs.acs.org.

References

(1) Tsien, R. W.; Wheeler, D. B. Voltage-Gated Calcium Channels. In *Calcium as a Cellular Regulator*; Carafoli, E., Klee, C., Eds.; Oxford University Press: New York, 1999; pp 171−199.

(2) (a) Ertel, E. A.; Campbell, K. P.; Harpold, M. M.; Hofmann, F.; Mori, Y.; Perez-Reyes, E.; Schwartz, A.; Snutch, T. P.; Tanabe, T.; Birnbaumer, L.; Tsien, R. W.; Catterall, W. A. Nomenclature of voltage-gated calcium channels. *Neuron* **2000**, *25*, 533–535. (b) Perez-Reyes, E. Molecular physiology of low-voltage-activated T-type calcium channels. *Physiol. Rev.* **2003**, *83*, 117–161.

(3) (a) Connolly, T. M.; Barrow, J. C. Drugs Active at T-Type Ca^{2+} Channels. In *Voltage-Gated Ion Channels as Drug Targets*; Triggle, D. J., Gopalakrishnan, M., Rampe, D., Zheng, W., Eds.; Methods and Principles in Medicinal Chemistry, Vol. 29; Wiley-VCH: Weinheim, Germany, 2006; pp 84−99. (b) Ertel, E. A. Pharmacology of Ca_v3 (T-Type) Channels. In *Calcium Channel Pharmacology*; McDonough, S. I., Ed.; Kluwer Academic/Plenum Publishers: New York, 2003; pp 183−236. (c) McGivern, J. G. Pharmacology and drug discovery for T-type calcium channels. *CNS Neurol Disord. Drug Targets* **2006**, *5*, 587–603. (d) Shin, H.-S.; Cheong, E.-J.; Choi, S.; Lee, J.; Na, H. S. T-Type Ca^{2+} channels as therapeutic targets in the nervous system. *Curr. Opin. Pharmacol.* **2008**, *8*, 33–41.

(4) (a) Llinás, R. R.; Ribary, U.; Jeanmonod, D.; Kronberg, E.; Mitra, P. P. Thalamocortical dysrhythmia: a neurological and neuropsychiatric syndrome characterized by magnetoencephalography. *Proc. Natl. Acad. Sci. U.S.A.* **1999**, *96*, 15222–15227. (b) Deleuze, C.; Huguenard, J. R. Distinct electrical and chemical connectivity maps in the thalamic reticular nucleus: potential roles in synchronization and sensation. *J. Neurosci.* **2006**, *26*, 8633–8645. (c) Contreras, D. The role of T-channels in the generation of thalamocortical rhythms. *CNS Neurol. Disord. Drug Targets* **2006**, *5*, 571–585. (d) Steriade, M.; McCormick, D. A.; Sejnowski, T. J. Thalamocortical oscillations in the sleeping and aroused brain. *Science* **1993**, *262*, 679–685.

(5) (a) Clozel, J.-P.; Ertel, S. I.; Ertel, E. A. Discovery and main pharmacological properties of mibefradil (Ro 40-5967), the first selective T-type calcium channel blocker. *J. Hypertens.* **1997**, *15*, S17–S25. (b) Oparil, S. Mibefradil, a T-channel-selective calcium channel antagonist. Clinical trials in hypertension. *Am. J. Hypertens.* **1998**, *11*, 88S–94S. (c) Massie, B. M. Mibefradil: a selective T-type calcium antagonist. *Am. J. Cardiol.* **1997**, *80*, 23I–32I.

(6) Mullins, M. E.; Horowitz, B. Z.; Linden, D. H. J.; Smith, G. W.; Norton, R. L.; Stump, J. Life-threatening interaction of mibefradil and β-blockers with dihydropyridine calcium channel blockers. *JAMA, J. Am. Med. Assoc.* **1998**, *280*, 157–158.

(7) Coulter, D. A.; Huguenard, J. R.; Prince, D. A. Characterization of ethosuximide reduction of low-threshold calcium current in thalamic neurons. *Ann. Neurol.* **1989**, *25*, 589–593.

(8) See Supporting Information for references to recent work on T-type calcium channel inhibitors.

(9) (a) See Supporting Information for assay details. (b) Xie, X.; Van Deusen, A. L.; Vitko, I.; Babu, D. A.; Davies, L. A.; Huynh, N.; Cheng, H.; Yang, N.; Barrett, P. Q.; Perez-Reyes, E. Validation of high throughput screening assays against three subtypes of Ca_v3 T-type channels using molecular and pharmacologic approaches. *Assay Drug Dev. Technol.* **2007**, *5*, 191–203.

(10) (a) Carmeliet, E; Mubagwa, K. Antiarrhythmic drugs and cardiac ion channels: mechanisms of action. *Prog. Biophys. Mol. Biol.* **1998**, *70*, 1–72. (b) Triggle, D. J. Calcium-channel antagonists: mechanisms of action, vascular selectivities, and clinical relevance. *Cleveland Clin. J. Med.* **1992**, *59*, 617–627.

(11) Raab, C. E.; Butcher, J. W.; Connolly, T. M.; Karczewski, J.; Yu, N. X.; Staskiewicz, S. J.; Liverton, N.; Dean, D. C.; Melillo, D. G. Synthesis of the first sulfur-35-labeled hERG radioligand. *Bioorg. Med. Chem. Lett.* **2006**, *16*, 1692–1695.

(12) Schoemaker, H.; Hicks, P. E.; Langer, S. Z. Calcium channel receptor binding studies for diltiazem and its major metabolites: functional correlation to inhibition of portal vein myogenic activity. *J. Cardiovasc. Pharmacol.* **1987**, *9*, 173–180.

(13) van Niel, M. B.; Collins, I.; Beer, M. S.; Broughton, H. B.; Cheng, S. K. F.; Goodacre, S. C.; Heald, A.; Locker, K. L.; MacLeod, A. M.; Morrison, D.; Moyes, C. R.; O'Connor, D.; Pike, A.; Rowley, M.; Russell, M. G. N.; Sohal, B.; Stanton, J. A.; Thomas, S.; Verrier, H.; Watt, A. P.; Castro, J. L. Fluorination of 3-(3-(piperidin-1-yl)propyl)indoles and 3-(3-(piperazin-1-yl)indoles gives selective human 5-HT_{1D} receptor ligands with improved pharmacokinetic profiles. *J. Med. Chem.* **1999**, *42*, 2087–2104.

(14) 6-Aza-6-*tert*-butyloxycabonyl-1-oxaspiro[2.5]octane (**6**) was prepared from 1-*tert*-butyloxycarbonyl-4-piperidone and trimethyl sulfoxonium iodide: Corey, E. J.; Chaykovsky, M. Methylenecyclohexane Oxide. *Organic Syntheses*; Wiley: New York, 1973; Collect. Vol. V, 1973; pp 755−757.

(15) Sattler, A.; Haufe, G. High regioselectivity in the alternative cleavage of terminal epoxides with different sources of nucleophilic fluoride. *J. Fluorine Chem.* **1994**, *69*, 185–190.

(16) See Supporting Information for an alternative synthesis of **8**.

(17) Preparation of 2,2-dimethyltetrahydropyran-4-one: (a) Liljebris, C.; Martinsson, J.; Tedenborg, L.; Williams, M.; Barker, E.; Duffy, J. E. S.; Nygren, A.; James, S. Synthesis and biological activity of a novel class of pyridazine analogues as non-competitive reversible inhibitors of protein tyrosine phosphatase 1B (PTP1B). *Bioorg. Med. Chem.* **2002**, *10*, 3197–3212. (b) 2,2-Dimethyltetrahydropyran-4-one was converted to **12** by Wittig homologation with (methoxymethyl)triphenylphosphonium chloride and hydrolysis of the resulting methyl enol ether with formic acid.

(18) See Supporting Information for the method of absolute configuration determination.

(19) Coenen, A. M. L.; Drinkenburg, W. H. I. M.; Inoue, M.; van Luijtelaar, E. L. J. M. Genetic models of absence epilepsy, with emphasis on the WAG/Rij strain of rats. *Epilepsy Res.* **1992**, *12*, 75–86.

(20) Tröster, A. I.; Woods, S. P.; Fields, J. A.; Lyons, K. E.; Pahwa, R.; Higginson, C. I. Neuropsychological deficits in essential tremor: an expression of cerebello-thalamo-cortical pathophysiology? *Eur. J. Neurol* **2002**, *9*, 143–151.

(21) Miwa, H. Rodent models of tremor. *Cerebellum* **2007**, *6*, 66–72.

(22) MDS Pharma Services, Assay 473500. http://www.mdsps.com/.

(23) See Supporting Information for $Na_v1.5$ electrophysiology measurements.

(24) Dai, G.; Haedo, R. J.; Warren, V. A.; Ratliff, K. S.; Bugianesi, R. M.; Rush, A.; Williams, M. E.; Herrington, J.; Smith, M. M.; McManus, O. B.; Swensen, A. M. A high-throughput assay for evaluating state-dependence and subtype selectivity of Ca_v2 calcium channel inhibitors. *Assay Drug Dev. Technol.* **2008**, *6*, 195−212.

(25) Stump, G. L.; Smith, G. R.; Tebben, A. J.; Jahansouz, H.; Salata, J. J.; Selnick, H. G.; Claremon, D. A.; Lynch, J. J. In vivo canine cardiac electrophysiologic profile of 1,4-benzodiazepene I_{Ks} blockers. *J. Cardiovasc. Pharmacol.* **2003**, *42*, 105–112.

(26) Hayashi, K.; Wakino, S.; Sugano, N.; Ozawa, Y.; Homma, K.; Saruta, T. Ca^{2+} channel subtypes and pharmacology in the kidney. *Circ. Res.* **2007**, *100*, 342–353.

(27) See Supporting Information for assay details.

JM800419W